Optomechanically induced entanglement

Xihua Yang,[1,*] Zhiyong Yin,[1] and Min Xiao[2]
[1]*Department of Physics, Shanghai University, Shanghai 200444, China*
[2]*Department of Physics, University of Arkansas, Fayetteville, Arkansas 72701, USA and National Laboratory of Solid State Microstructures and School of Physics, Nanjing University, Nanjing 210093, China*

(Received 28 August 2018; published 4 January 2019)

We present a special quantum phenomenon named optomechanically induced entanglement in the conventional single-cavity optomechanical system driven by a strong pump input field and a relatively weak probe input field. Bipartite entanglement between the pump and probe output fields can be achieved under realistic experimental conditions when the input pump (probe) field is blue detuned by the mechanical frequency (resonant) with respect to the cavity field. The physical origin is the mechanical oscillator displacement, which plays a role similar to the atomic coherence for the well-known electromagnetically induced transparency in the traditional Λ-type atomic system. This scheme provides an alternative, convenient way to generate nondegenerate entangled bright light beams by using only coherent laser fields, and may bring great facility in realistic quantum information processing protocols.

DOI: 10.1103/PhysRevA.99.013811

I. INTRODUCTION

Electromagnetically induced transparency (EIT), initially discovered in atomic systems [1–4], has proven to be a convenient and efficient means for many different applications, such as the production of slow light and giant nonlinear effects [5,6], quantum memory [7,8], and the generation of quantum entanglement [9–16]. The existence of the analog of EIT in the optomechanical system, that is, optomechanically induced transparency (OMIT), has also been theoretically studied and experimentally demonstrated [17–21], which has potential applications in control of light speed [20], quantum router [22], charge measurement [23], light storage [24], etc. Moreover, the opposite effects, i.e., electromagnetically induced absorption (EIA) [25,26] and optomechanically induced absorption (OMIA) [19] have been examined as well. The origin of these phenomena is quantum coherence and interference. However, in all of the above treatments of the interaction between the laser fields and matter, only the mean response of the system to the weak probe field in the presence of the strong pump field is considered, whereas the quantum fluctuations of the pump and probe fields are ignored. Recently, we have taken into account the quantum fluctuations of both the laser fields and atomic operators, and demonstrated electromagnetically induced entanglement (EIE) in the simple Λ-type atomic system driven by a strong pump field and a relatively weak probe field [16]. Here, we further show that optomechanically induced entanglement (OMIE) can be realized in the traditional single-cavity optomechanical system driven by a strong pump input field and a relatively weak probe input field with the consideration of the quantum fluctuations of the laser fields and mirror vibrating mode. It is clear that bipartite entanglement between the pump and probe output fields can be achieved with the realistic experimental conditions when the input pump (probe) field is blue detuned by the mechanical frequency (resonant) with respect to the cavity field.

The present scheme is quite different from those for generating two [27,28] or multiple [29] entangled output fields with a single-cavity optomechanical system. In Ref. [27], Genes *et al.* demonstrated that the entanglement between the Stokes and anti-Stokes sidebands of a single driving field can be achieved with an optomechanical system; however, the vibrating mirror is only entangled with the Stokes field and not entangled with the anti-Stokes field. It is shown in Ref. [28] that the Einstein-Podolsky-Rosen (EPR)-type entanglement can be obtained via radiation pressure by using two degenerate orthogonally polarized laser beams with equal intensity, whereas in Ref. [29], multiple entangled laser fields can be achieved in a cavity optomechanical system by using multiple fields with each field driving a corresponding longitudinal mode of the cavity field. The distinct advantage of the present scheme is that bipartite entanglement between the nondegenerate pump and probe output fields can be achieved with the pump and probe input fields driving a single longitudinal mode of the cavity field, which leads to the special OMIE effect; moreover, the vibrating mirror is entangled with both the pump and probe output fields.

II. THEORETICAL MODEL AND HEISENBERG-LANGEVIN EQUATIONS

Figure 1(a) schematically shows the considered conventional single-cavity optomechanical system driven by a strong pump input field and a relatively weak probe input field and their corresponding outputs, which is composed of a fixed (partially transmitting) mirror and a vibrating (perfectly reflecting) mirror coupled to a longitudinal mode of the cavity field due to radiation pressure force [17,18]. As displayed in Fig. 1(b), we assume that the input pump laser field with frequency ω_c is blue detuned by the mechanical oscillation frequency to the cavity field, and the input probe field with

*yangxh@shu.edu.cn

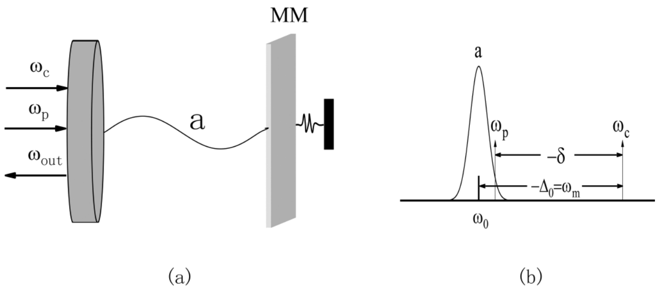

FIG. 1. (a) The considered conventional single-cavity optomechanical system with a movable mirror (MM) driven by a strong pump (ω_c) input field and a relatively weak probe (ω_p) input field and their corresponding outputs, where a represents the longitudinal cavity field mode with frequency ω_0. (b) The relevant frequencies of the pump, probe, and cavity fields, and the corresponding frequency detuning of the cavity (probe) field with respect to the input pump laser field denoted by $\Delta_0 = \omega_0 - \omega_c$ ($\delta = \omega_p - \omega_c$), where the input probe field is tuned around the cavity resonance frequency with $\Delta_0 = -\omega_m$.

frequency ω_p is tuned around the cavity resonance frequency. The Hamiltonian of the system can be expressed as [17,18]

$$H = \hbar\omega_0 a^+ a + \hbar\omega_m b^+ b - \hbar g_0 a^+ a(b^+ + b) + i\hbar\eta_c(a^+ e^{-i\omega_l t} - a e^{i\omega_l t}) + i\hbar\eta_p(a^+ e^{-i\omega_p t} - a e^{i\omega_p t}), \tag{1}$$

where a (a^+) is the annihilation (creation) operator of the cavity field mode with frequency ω_0 and decay rate k; b (b^+) is the annihilation (creation) operator of the mechanical oscillation mode with oscillation frequency $\omega_{\rm m}$ and mechanical damping rate $\gamma_{\rm m}$; $g_0 = \omega_0\sqrt{\hbar/m\omega_m}/L$ is the optomechanical coupling coefficient of the radiation pressure with L being the cavity length, and m the effective mass of the mechanical oscillator. The last two terms in Eq. (1) describe the input driving pump and probe laser fields and their interaction with the cavity field mode; $\eta_{c(p)}$ is related to the input pump (probe) field power $P_{c(p)}$ with $\eta_{c(p)} = \sqrt{2P_{c,p}k/\hbar\omega_0}$. In the frame rotating at the input pump field frequency ω_c, the Heisenberg-Langevin equations can be written as

$$\dot{a} = -(k + i\Delta_0)a + ig_0 a(b + b^+) + \eta_{\rm c} + \eta_p e^{-i\delta t} + \sqrt{2k}a^{\rm in}, \tag{2a}$$

$$\dot{b} = -(\gamma_m + i\omega_m)b + ig_0 a^+ a + \sqrt{2\gamma_m}b^{\rm in}, \tag{2b}$$

where $\Delta_0 = \omega_0 - \omega_c$ ($\delta = \omega_p - \omega_c$) is the frequency detuning of the cavity (probe) field with respect to the input pump laser field; $a^{\rm in}(t)$ and $b^{\rm in}(t)$ are the optical and mechanical noise operators with the relevant nonzero correlation functions $\langle a^{\rm in}(t)a^{in+}(t')\rangle = \delta(t-t')$ and $\langle b^{\rm in}(t)b^{in+}(t')\rangle = (n+1)\delta(t-t')$ in the limit of large mechanical quality factor (i.e., $Q_m = \omega_m/\gamma_m \gg 1$ [30]), where $\bar{n} = 1/[\exp(h\omega_m/k_B T) - 1]$ is the mean thermal phonon number with k_B being the Boltzmann constant and T the mirror temperature. As in the OMIT scheme [17–20], we assume that the pump field strength is far larger than that of the probe field (i.e., $P_c \gg P_p$), so the mechanical excitation mainly results from the pump field, and the radiation pressure force from the probe field can be safely neglected; consequently, in the resolved sideband regime (i.e., $\omega_m \gg \kappa$), solutions to Eqs. (2a) and (2b) can be well approximately by the ansatz $a = a_0 + a_+ e^{-i\delta t} + a_- e^{i\delta t}$ and $b \doteq b_0$, where a_0, a_+, and a_- correspond to the cavity field operators with frequency components of the pump (ω_c), probe (ω_p), and four-wave-mixing fields ($2\omega_c - \omega_p$) in the original frame, respectively. A similar treatment has been performed by Vitali *et al.* [31] with a proposed experimental readout scheme to measure the generated optomechanical entanglement by employing an additional adjacent cavity sharing the common vibrating mirror, where since the probe field is far weaker than the coupling field, its back action on the mechanical mode is neglected and the mirror dynamics is safely thought to be determined only by the strong coupling field, corresponding just to the above approximation of $b \doteq b_0$. Note also that a similar treatment has been employed in Ref. [32] to generate nanomechanical squeezing with a parametrically driven nanomechanical resonator capacitively coupled to a microwave cavity. Substituting a and b into Eqs. (2a) and (2b) and equating the frequency components, the evolutions of the operators a_0, a_+, and b_0 can be written as

$$\dot{a}_0 = -(k + i\Delta_0)a_0 + ig_0 a_0(b_0 + b_0^+) + \eta_{\rm c} + \sqrt{2k}a_0^{\rm in}, \tag{3a}$$

$$\dot{a}_+ = -[k + i(\Delta_0 - \delta)]a_+ + ig_0 a_+(b_0 + b_0^+) + \eta_p + \sqrt{2k}a_+^{\rm in}, \tag{3b}$$

$$\dot{b}_0 = -(\gamma_m + i\omega_m)b_0 + ig_0 a_0^+ a_0 + \sqrt{2\gamma_m}b^{\rm in}, \tag{3c}$$

where in Eq. (3c) we neglect the optomechanical coupling of the radiation pressure from the probe and four-wave-mixing fields since their intensities are far weaker than that of the pump field. Also, the evolution of the operator a_- is not written out in the above expressions as we only examine the entangled feature between the pump and probe output fields as well as the mirror. In fact, by comparing Eqs. (3a)–(3c) to Eqs. (2a)–(2c) and Eq. (13) in Ref. [31], it can be clearly seen that the probe field in the present scenario has similar features as the probe field driving an additional adjacent cavity, used in Ref. [31], to detect the optomechanical entanglement. By writing each Heisenberg operator as the sum of its steady-state mean value and a small fluctuation operator with zero-mean value, $a_{0,+} = \alpha_{0,+} + \delta a_{0,+}$, $b_0 = \beta + \delta b$, the steady-state mean values can be easily obtained by letting the time derivatives be equal to zero and neglecting the noise operators in Eqs. (3a)–(3c), and one can get $\alpha_0 = \eta_c/|k + i[\Delta_0 - g_0(\beta + \beta^*)]|$, $\beta = ig_0|\alpha_0|^2/(\gamma_m + i\omega_m)$, and $\alpha_+ = \eta_p/\{k + i[\Delta_0 - \delta - g_0(\beta + \beta^*)]\}$, where we have chosen the phase reference of the driving field so that a_0 is real and positive. Defining the fluctuation quadrature operators, $\delta X_{0,+} = (\delta a_{0,+} + \delta a_{0,+}^+)/\sqrt{2}$ and $\delta Y_{0,+} = (\delta a_{0,+} - \delta a_{0,+}^+)/\sqrt{2}i$, and $\delta X_b = (\delta b + \delta b^+)/\sqrt{2}$ and $\delta Y_b = (\delta b - \delta b^+)/\sqrt{2}i$, and the corresponding Hermitian noise operators, $X_m^{\rm in} = (a_m^{\rm in} + a_m^{in+})/\sqrt{2}$ and $Y_m^{\rm in} = (a_m^{\rm in} - a_m^{in+})/\sqrt{2}i$ ($m = 0, +$), and $X_b^{\rm in} = (b^{\rm in} + b^{in+})/\sqrt{2}$ and $Y_b^{\rm in} = (b^{\rm in} - b^{in+})/\sqrt{2}i$, we can obtain the quantum

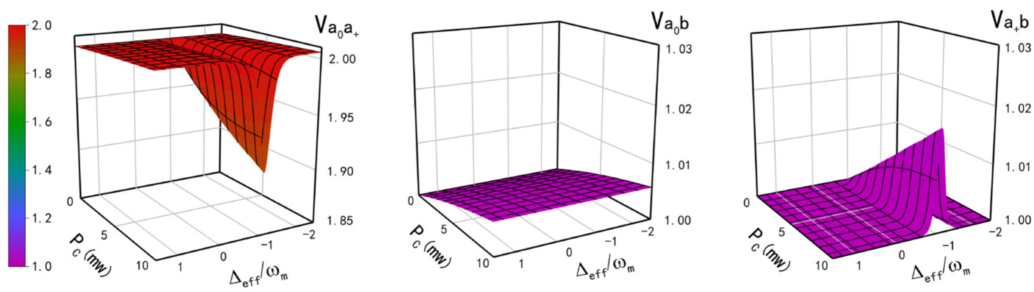

(a) (b) (c)

FIG. 2. The 3D plots of the evolution of the correlations $V_{a_0a_+}$ (a), V_{a_0b} (b), and V_{a_+b} (c) at zero Fourier frequency as a function of the input pump field power P_c and frequency detuning δ of the probe field to the pump field, where we set $\Delta_0 = -\omega_m$ and use the realistic experimental parameters in Ref. [34] with $L= 0.025$ m, $T = 0.01$ K, $\omega_m = 2\pi \times 947$ kHz, $\gamma_m = 2\pi \times 141$ Hz, $\kappa = 2\pi \times 215$ kHz, $\lambda = 1064$ nm, $m= 145 \times 10^{-12}$ kg, and $P_c = 100P_p$.

Langevin equations for the fluctuation operators:

$$\delta\dot{X}_0 = -k\delta X_0 + [\Delta_0 - g_0(\beta + \beta^*)]\delta Y_0 + \sqrt{2k}X_0^{\text{in}}, \tag{4a}$$

$$\delta\dot{Y}_0 = -k\delta Y_0 - [\Delta_0 - g_0(\beta + \beta^*)]\delta X_0 + 2g_0\alpha_0\delta X_b + \sqrt{2k}Y_0^{\text{in}}, \tag{4b}$$

$$\delta\dot{X}_+ = -k\delta X_+ + [\Delta_0 - \delta - g_0(\beta + \beta^*)]\delta Y_+ - 2g_0\text{Im}\alpha_+\delta X_b + \sqrt{2k}X_+^{\text{in}}, \tag{4c}$$

$$\delta\dot{Y}_+ = -k\delta Y_+ - [\Delta_0 - \delta - g_0(\beta + \beta^*)]\delta X_+ + 2g_0\text{Re}\alpha_+\delta X_b + \sqrt{2k}Y_+^{\text{in}}, \tag{4d}$$

$$\delta\dot{X}_b = -\gamma_m\delta X_b + \omega_m\delta Y_b + \sqrt{2\gamma_m}X_b^{\text{in}}, \tag{4e}$$

$$\delta\dot{Y}_b = -\gamma_m\delta Y_b - \omega_m\delta X_b + 2g_0\alpha_0\delta X_0 + \sqrt{2\gamma_m}Y_b^{\text{in}}. \tag{4f}$$

By Fourier-transforming the Heisenberg-Langevin equations (4a)–(4f), the quantum fluctuations of the operators with respect to the Fourier frequency ω can be attained. The quantum fluctuations of the output fields can be obtained by using the input-output relation $\delta A_{0,+}^{\text{out}}(\omega) = \sqrt{2k}\delta A_{0,+}(\omega) - A_{0,+}^{\text{in}}(\omega)$ $(A = X, Y)$. In the following, we will focus on the entanglement at $\omega = 0$, as it describes the quantum correlations of the output modes with frequencies corresponding to the pump and probe fields. In this case, the fluctuation quadrature operators are Hermitian, and we can use the entanglement criterion $V_{a_0a_+} = \langle\delta U(\omega)\delta U^+(\omega) + \delta V(\omega)\delta V^+(\omega)\rangle < 2$ proposed in Refs. [33–35] to test the entanglement feature between the output pump and probe fields, where $\delta U(\omega) = \delta X_0^{\text{out}}(\omega) + \delta X_+^{\text{out}}(\omega)$ and $\delta V(\omega) = \delta Y_0^{\text{out}}(\omega) - \delta Y_+^{\text{out}}(\omega)$. Satisfying the above inequality is a sufficient demonstration for the generation of bipartite entanglement, and the smaller the correlation $V_{a_0a_+}$ is, the stronger the degree of the bipartite entanglement becomes. We consider the realistic experimental parameters in Ref. [36], which has also been used in the theoretical paper on OMIT [17]. According to Ref. [36], the relevant parameters are set as $L = 0.025$ m, $T = 0.01$ K, $\omega_m = 2\pi \times 947$ kHz, $\gamma_m = 2\pi \times 141$ Hz, $\kappa = 2\pi \times 215$ kHz, $\lambda = 1064$ nm, $m = 145 \times 10^{-12}$ kg, $P_c = 100P_p$, and $\Delta_0 = -\omega_m$. Note that similar results can also be obtained with the experimental feasible parameters in Ref. [18], that is, $L = 0.032$ mm, $T = 0.01$ K, $\omega_m = 2\pi \times 51.8$ MHz, $\gamma_m = 2\pi \times 41$ kHz, $\kappa = 2\pi \times 15$ MHz, $\lambda = 775$ nm, and $m = 20 \times 10^{-12}$ kg. Within these chosen parameter regimes, we have numerically confirmed the validity of the above-mentioned approximations made in linearizing dynamics of the system, and numerically confirmed that the stability conditions of the system derived by applying the Routh-Hurwitz criterion [37] are satisfied

III. RESULTS AND DISCUSSIONS

Generation of OMIE. Figure 2(a) gives the main results of this study, where the three-dimensional (3D) plot of the evolution of the correlation $V_{a_0a_+}$ at zero Fourier frequency as a function of the input pump field power P_c and frequency detuning δ of the probe field with respect to the pump field is depicted. Obviously, when the input pump field is blue detuned by the mechanical frequency with respect to the cavity field (i.e., $\Delta_0 = -\omega_m$) and its intensity is very weak, $V_{a_0a_+}$ is nearly equal to 2 in the whole range of the detuning δ; that is, no entanglement exists between the output probe and pump fields. With the increase of the input pump field intensity, there exists a narrow dip in a limited range of the detuning δ with the minimum value becoming smaller than 2 at about $\delta = -\omega_m$, which demonstrates the generation of genuine bipartite entanglement between the pump and probe output fields. Moreover, within the experimental feasible parameter range, the larger the input pump field intensity, the deeper the narrow dip and the stronger the bipartite entanglement between the two output fields, which characterizes the existence of the OMIE. For comparison, we show in Figs. 2(b) and 2(c) the evolutions of the correlations V_{a_0b} and V_{a_+b} at zero Fourier frequency as functions of P_c and δ with $\Delta_0 = -\omega_m$. It can be seen that V_{a_0b} and V_{a_+b} are both nearly equal to 1 over the same variation ranges of P_c and δ as in Fig. 2(a), indicating that the probe and pump output fields are both entangled with the mirror, except that entanglement sharing would exist among the subsystems with the increase of the input pump field power P_c at about $\delta = -\omega_m$; that is, the bipartite entanglement between the two output fields can be efficiently generated and enhanced at the

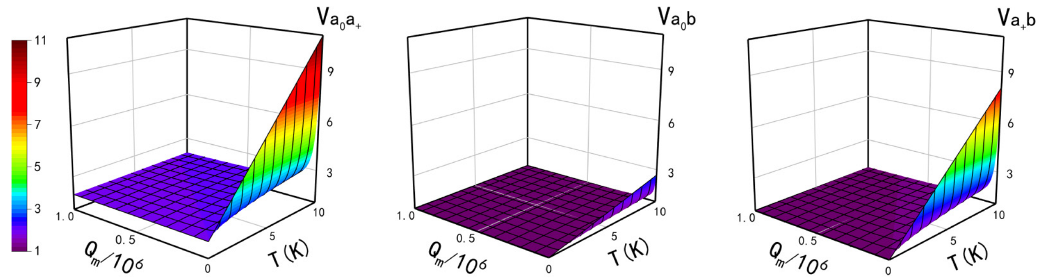

(a) (b) (c)

FIG. 3. The 3D plots of the evolution of the correlations $V_{a_0a_+}$ (a), V_{a_0b} (b), and V_{a_+b} (c) at zero Fourier frequency with respect to the environmental temperature T and quality factor Q_m of the vibrating mirror mode with $\Delta_0 = \delta = -\omega_m$, $P_c = 5$ mW; the other parameters are the same as those in Fig. 2.

expense of the bipartite entanglement between the mirror and the two output fields with increasing P_c. Note that in the above experimentally feasible range of the input pump field power, no entanglement exists between the two output fields when the input pump field is red detuned by the mechanical resonance frequency with respect to the cavity field and the probe field is tuned to the cavity resonance frequency, which is due to the employed relatively weak input pump field intensity. The similar input field power dependence of entanglement generation with an optomechanical system driven by a single laser field in the red- and blue-detuned regimes has been examined by Genes *et al.* [27].

As is well known, the environmental temperature and quality factors of the cavity field ($Q = \omega_0/\kappa$) and vibrating mirror ($Q_m = \omega_m/\gamma_m$) play important roles in the entanglement generation in an optomechanical system. Figure 3(a) displays the 3D plot of the evolution of the correlation $V_{a_0a_+}$ at zero Fourier frequency with respect to the environmental temperature T and quality factor Q_m of the vibrating mirror mode with the experimentally available parameters, where the variation of Q_m is obtained by varying the mechanical damping rate γ_m of the vibrating mirror. Note that as $C = 4g_0^2\alpha_0^2/\kappa\gamma_m$, the variation of γ_m corresponds to the change of the cooperativity C. It can be seen from Fig. 3(a) that, when the mechanical quality factor Q_m is very small and the environmental temperature is high, the correlation $V_{a_0a_+}$ is much larger than 2, and no bipartite entanglement between the pump and probe output fields can be achieved. With the increase of the quality factor Q_m and/or decrease of the environmental temperature, the correlation $V_{a_0a_+}$ becomes smaller than 2, indicating the genuine bipartite entanglement between the pump and probe output fields can be produced. The lower the environmental temperature and/or the larger the quality factor Q_m within the experimentally practical region, the stronger the bipartite entanglement between the pump and probe output fields. The evolution of the correlations V_{a_0b} and V_{a_+b} at zero Fourier frequency with respect to T and Q_m exhibits similar behavior as that of the correlation $V_{a_0a_+}$ in Fig. 3(a) [see Figs. 3(b) and 3(c)]. It is worth noting that, as shown in Fig. 3(a), although the bipartite optomechanical entanglement between the output pump and probe fields would be weakened dramatically with the increase of the mirror temperature, it still persists for the temperature above 9 K with the experimentally accessible high-Q mechanical resonator of the vibrating mirror (e.g., $Q_m = 10^6$ in Ref. [21]), whereas the bipartite entanglements between the mirror and two output fields exhibit strong robustness to the environmental temperature, and can still exist even at high (e.g., 100 K or higher) temperature. Note also that results similar to those in Figs. 3(a)–3(c) can be obtained by varying κ and T with fixed γ_m and P_c.

Mechanism of OMIE. To get a physical insight into the predicted OMIE, it is instructive to consider the interaction between the cavity field and vibrating mirror. As shown in Fig. 1, when the input pump field is blue detuned by the mechanical resonance frequency with respect to the cavity field, the radiation pressure of the strong pump beam, impinging on the mechanical oscillator, produces optomechanical coupling between the vibrational mode and the Stokes sideband mode in the resolved-sideband regime. In this case, the effective interaction Hamiltonian can be described by a parametric-type interaction $H_I = \hbar g_0(a_0^+ b^+ + a_0 b)$ [21,27], which results in the bipartite entanglement between the vibrational mode and cavity field and the subsequent entanglement between the output pump field and vibrating mirror. When a much weaker input probe field is incident onto the cavity with frequency near the cavity resonance, i.e., $\delta = \Delta_0 - g_0(\beta + \beta^*)$, the fluctuation quadrature operators of the output probe field at zero Fourier frequency can be expressed as $\delta X_+^{\text{out}} = -\frac{2\sqrt{2}g_0\text{Im}\alpha_+}{\sqrt{k}}\delta X_b + X_+^{\text{in}}$ and $\delta Y_+^{\text{out}} = \frac{2\sqrt{2}g_0\text{Re}\alpha_+}{\sqrt{k}}\delta X_b + Y_+^{\text{in}}$ with $\delta X_b = \frac{\omega_m}{\gamma_m}\delta Y_b + \frac{\sqrt{2}}{\sqrt{\gamma_m}}X_b^{\text{in}}$ by solving Eqs. (4c)–(4e). The above expressions indicate that the output mode of the probe field can fully characterize the property of the mechanical oscillation mode, thereby getting entangled with the vibrating mirror and subsequently with the output pump field. In this regard, the function of the probe field has a feature similar to the probe field used in Ref. [31] to detect the optomechanical entanglement by using an additional adjacent cavity sharing the common vibrating mirror.

The physical mechanism underlying the generated bipartite entanglement between the output pump and probe fields can also be seen clearly from Eqs. (3a)–(3c). As shown in Eqs. (3a)–(3c), the pump and probe field modes are both optomechanically coupled to the mechanical oscillation mode via the mechanical displacement operator X_b and interact with each other; subsequently correlation and entanglement between the two fields, as well as the corresponding two output fields, can be established. In this respect, the mechanical oscillator displacement plays a role similar to the atomic spin coherence for generating multipartite entanglement in the Λ-type EIT configuration [14,15], which is the origin of the produced OMIE.

IV. SUMMARY

In conclusion, we have shown optomechanically induced entanglement in the conventional single-cavity optomechanical system driven by a strong off-resonant pump input field and a relatively weak near-resonant probe input field. Bipartite entanglement between the pump and probe output fields can be achieved with the realistic experimental parameters when the input pump (probe) field is blue detuned by the mechanical frequency (resonant) with respect to the cavity field. Unlike the atomic systems which rely on particular frequencies corresponding to naturally existing resonances, the optomechanical system can, in principle, couple to light fields with any frequencies, thereby providing a convenient and efficient way for generating nondegenerate narrow-band continuous-variable entangled fields with any desired wavelengths by using only coherent input laser fields, which may find promising applications in realistic quantum network and quantum information processing.

ACKNOWLEDGMENTS

This work is supported by the National Natural Science Foundation of China (Grants No. 11574195 and No. 61435007), the Innovation Action Plan of International Academic Cooperation and the Exchange Program of the Shanghai Municipal Science and Technology Commission (Grant No. 16520720800).

[1] K. J. Boller, A. Imamoglu, and S. E. Harris, Phys. Rev. Lett. **66**, 2593 (1991).
[2] M. Xiao, Y. Q. Li, S. Z. Jin, and J. Gea-Banacloche, Phys. Rev. Lett. **74**, 666 (1995).
[3] S. E. Harris, Phys. Today **50**(7), 36 (1997).
[4] M. Fleischhauer, A. Imamoglu, and J. P. Marangos, Rev. Mod. Phys. **77**, 633 (2005).
[5] A. Kasapi, M. Jain, G. Y. Yin, and S. E. Harris, Phys. Rev. Lett. **74**, 2447 (1995).
[6] L. V. Hau, S. E. Harris, Z. Dutton, and C. H. Behroozi, Nature **397**, 594 (1999).
[7] M. Fleischhauer and M. D. Lukin, Phys. Rev. Lett. **84**, 5094 (2000).
[8] M. D. Lukin and A. Imamoglu, Nature **413**, 273 (2001).
[9] L. M. Duan, M. D. Lukin, J. I. Cirac, and P. Zoller, Nature **414**, 413 (2001).
[10] C. H. van der Wal, M. D. Eisaman, A. Andre, R. L. Walsworth, D. F. Phillips, A. S. Zibrov, and M. D. Lukin, Science **301**, 196 (2003).
[11] A. Kuzmich, W. P. Bowen, A. D. Boozer, A. Boca, C. W. Chou, L. M. Duan, and H. J. Kimble, Nature **423**, 731 (2003).
[12] V. Boyer, A. M. Marino, R. C. Pooser, and P. D. Lett, Science **321**, 544 (2008).
[13] A. M. Marino, R. C. Pooser, V. Boyer, and P. D. Lett, Nature **457**, 859 (2009).
[14] X. H. Yang, B. L. Xue, J. X. Zhang, and S. Y. Zhu, Sci. Rep. **4**, 6629 (2014).
[15] X. H. Yang, Y. Y. Zhou, and M. Xiao, Phys. Rev. A **85**, 052307 (2012).
[16] X. H. Yang and M. Xiao, Sci. Rep. **5**, 13609 (2015).
[17] G. S. Agarwal and S. Huang, Phys. Rev. A **81**, 041803 (2010).
[18] S. Weis, R. Rivière, S. Deléglise, E. Gavartin, O. Arcizet, A. Schliesser, and T. J. Kippenberg, Science **330**, 1520 (2010).
[19] J. D. Teufel, D. Li, M. S. Allman, K. Cicak, A. J. Sirois, J. D. Whittaker, and R. W. Simmonds, Nature **471**, 204 (2011).
[20] A. H. Safavi-Naeini, T. P. Mayer Alegre, J. Chan, M. Eichenfield, M. Winger, Q. Lin, J. T. Hill, D. E. Chang, and O. Painter, Nature **472**, 69 (2011).
[21] M. Aspelmeyer, T. J. Kippenberg, and F. Marquardt, Rev. Mod. Phys. **86**, 1391 (2014), and references therein.
[22] G. S. Agarwal and S. Huang, Phys. Rev. A **85**, 021801 (2012).
[23] J.-Q. Zhang, Y. Li, M. Feng, and Y. Xu, Phys. Rev. A **86**, 053806 (2012).
[24] D. E. Chang, A. H. Safavi-Naeini, M. Hafezi, and O. Painter, New J. Phys. **13**, 023003 (2011).
[25] A. Lezama, S. Barreiro, and A. M. Akulshin, Phys. Rev. A **59**, 4732 (1999).
[26] X. H. Yang, J. T. Sheng, and M. Xiao, Phys. Rev. A **84**, 043837 (2011).
[27] C. Genes, A. Mari, P. Tombesi, and D. Vitali, Phys. Rev. A **78**, 032316 (2008).
[28] V. Giovannetti, S. Mancini, and P. Tombesi, Eur. Phys. Lett. **54**, 559 (2001).
[29] S. Giannini, S. Mancini, and P. Tombesi, Quantum Inf. Comput. **3**, 265 (2003).
[30] R. Benguria and M. Kac, Phys. Rev. Lett. **46**, 1 (1981).
[31] D. Vitali, S. Gigan, A. Ferreira, H. R. Böhm, P. Tombesi, A. Guerreiro, V. Vedral, A. Zeilinger, and M. Aspelmeyer, Phys. Rev. Lett. **98**, 030405 (2007).
[32] M. J. Woolley, A. C. Doherty, G. J. Milburn, and K. C. Schwab, Phys. Rev. A **78**, 062303 (2008).
[33] L. M. Duan, G. Giedke, J. I. Cirac, and P. Zoller, Phys. Rev. Lett. **84**, 2722 (2000).
[34] D. Vitali, G. Morigi, and J. Eschner, Phys. Rev. A **74**, 053814 (2006).
[35] Q. Glorieux, R. Dubessy, S. Guibal, L. Guidoni, J.-P. Likforman, T. Coudreau, and E. Arimondo, Phys. Rev. A **82**, 033819 (2010).
[36] S. Gröblacher, K. Hammerer, M. R. Vanner, and M. Aspelmeyer, Nature **460**, 724 (2009).
[37] E. X. DeJesus and C. Kaufman, Phys. Rev. A **35**, 5288 (1987).